CIENCIA 14(4), 440 - 451, 2006
Maracaibo, Venezuela

Influence of the dynamical parameters and viral mutability in the progression of HIV-1 infection

Horacio Ortega

Cátedra de Física, Universidad Experimental Politécnica Antonio José de Sucre, VR La Yaguara, Caracas. A.P. 47636 Los Chaguaramos, Caracas, 1041-A, Venezuela

Recibido: 21-06-05 Aceptado: 15-11-06

Abstract

We use the concepts of immunodominance and antigenic oscillation for describing a model of HIV-1infection. We consider not only mutating virions and T-CD4 cells, but also viral reservoirs as macrophages and follicular dendritic cells (FDPC). We also consider strong cytotoxic attack against reservoirs and the extra cellular attack on virions, both coordinated by T-CD4 cells. We simulate mutations by a Montecarlo routine. Virus high mutability impairs the immune system by nullifying the assumed attack by immune cells (CTL) to infected reservoirs. Additionally our results show that tackling virus invasion and posterior output from reservoirs could be an important alternative in therapy.

Key words: Cytolithic cells; equilibrium point; mutability; reservoirs; viral escape.

Influencia de los parámetros dinámicos y la mutabilidad viral en la progresión de la infección por VIH-1

Resumen

Se utiliza los conceptos de inmunodominancia y oscilación antigénica para desarrollar un modelo de infección por VIH-1. Se considera el efecto no solo de viriones mutantes y células T-CD4, sino también de reservorios virales, como macrófagos y células foliculares dendríticas entre otros. También se considera ataque citotóxico contra los reservorios y ataque extracelular sobre los viriones, ambos coordinados por las células T-CD4. Las mutaciones se simulan mediante una rutina de Montecarlo. La alta mutabilidad del virus desequilibra al sistema inmunológico, al anular el supuesto ataque de las células inmunitarias (CTL) a los reservorios infectados. Adicionalmente nuestros resultados muestran que bloquear la invasión del virus a los reservorios, y la posterior producción de viriones desde dichos santuarios, podría ser una alternativa importante en terapia.

Palabras clave: Células citolíticas; escape viral; mutabilidad; punto de equilibrio; reservorios.

* E-mail: palacu49@hotmail.com

1. Introduction

The acquired immunodeficiency syndrome goes on as the major threat ever posed to the world public health. Additionally to impairing the immune system interactions by storming T-CD4 cells, HIV-1 infects in a no *Cytopathic* way immune long lived cells, among them, macrophages (1, 2, 3) memory and resting T-cells (3), and lymphoid tissue (4, 5, 6). Dendritic cells can also be directly invaded by VIH-1 (7). Some indirect mechanisms of invasion to T-CD4 cells, as those mediated by dendritic cells (7, 8) or by viral genomes (9) seem to be very perverse ones. Curiously, a lacking of correlation between the lifetime of the infected cells and T-CD4 counts has been reported (10). The immune system can check HIV-1 neutralizing free virions (11, 12, 13), by lymphocyte mediated control of viral progression, (14, 15), by destruction of infected cells displaying viral epitopes, a fact inferred by the emergence of an anti HIV-CTL response in the early stages of the infection (16, 17), and also by the so-called biphasic decay (18). Cytotoxic cells can also pour soluble anti VIH-1 factors into the blood stream (19). However, cytotoxic activity of CTL in blood needs continue stimulation (20), and also the presence of long lived memory CTL cells (21). Persistence of viral replication is also required for maintaining high frequencies of CTL effectors (22). Some aspects of the interaction virions-anti HIV cells are elsewhere discussed (23, 24). The eventual failure of the immune system could be explained as a consequence of the high viral mutability, but also by the existence of resistant strains of virions, or slowly replying ones (25). The antibody mediated response is a subject that deserves attention, especially by the possibility of vaccine design (26, 27), and also because there exist known mechanisms for viral escape from humoral attack (28, 29), or by affording the invasion of virions to macrophages by means of their IgC Fc receptor fragment. At the advanced stages of the illness the immune system collapses and opportunistic infections emerge inducing the death of the infected organism. These stages are characterized by an notable increase in the viral burden, although the currently accepted source of virions, T-CD4 cells is depressed, a fact that highlights the need for additional sources of virions as B lymphocytes (30), splenocytes (31) or follicular dendritic cells (4).

Mathematical modelling should allow acquiring a better knowledge of complex dynamics so that the decisive factors in the struggle of the VIH-1 and the immune system become finally established. There is a wealth of models of the VIH-1-immune system interaction, and we mention here just the works by De Boer and Perelson (32), and Wodarz and Nowak (33). A revision of the state-of-the-art in modeling VIH-1–immune system interaction can be found in (34), therefore we remit there to lectors interested in such topics.

In this work we build various spaces of parameters related to the immune response, the viral mutability, and the presence of cytolytic cells. It should be clear that the presence of known viral reservoirs, until yet not considered, defines the step control-progression of the illness, and that it should be important designing therapies maintaining this control. We discuss in section 2 fundamentals of our model, its stability, and how we include the effect of mutations and opportunistic infections on its behavior. In section 3 we show the results of several numerical integrations. The influence of the immune attack on virions, and also the viral escape produced by high viral mutability is explicitly considered. In section 4 we make a discussion of our results and present our conclusions. We used AUTOCAD 2000 for tracing the Figure 1; SIGMAPLOT 5.05 for the Figures 2, 4, and 9, and routines from MATLAB 5.3 for the remaining ones.

2. The model

2.1. Fundamentals

We use in this paper a generalization (35) of a model originally proposed by Nowak et al. (36) for describing the evolution of AIDS

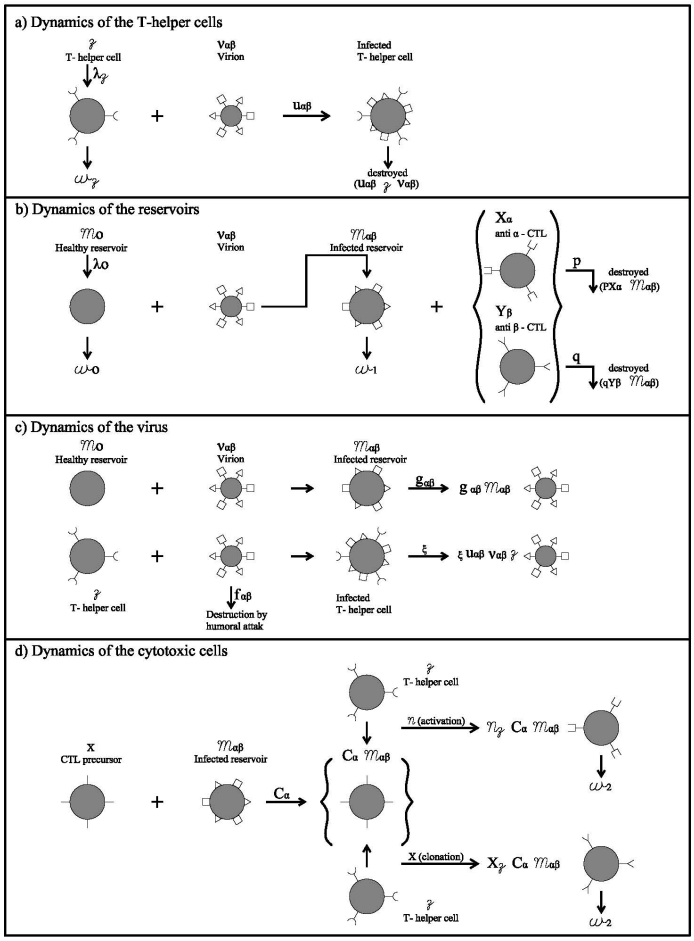

Figure 1. a) z, T-helper cells, $\nu_{\alpha\beta}$, virus, λ_z, T-helper cells creation rate, $(\omega_z)^{-1}$, T-helper cells lifetime. In absence of any other interaction the T-helper cells equilibrium density is $z^* = \lambda_z / \omega_z$. Virions destroy T-helper cells at a rate $u_{\alpha\beta}\, \nu_{\alpha\beta}\, z$. The full variation rate of the T-helper cells is $\lambda_z - u_{\alpha\beta}\, \nu_{\alpha\beta}\, z - \omega_z\, z$. b) m_0, healthy reservoirs, $m_{\alpha\beta}$, infected reservoirs, x_α, cytotoxic cells against the epitope α, (y_β, cytotoxic cells against the epitope β), λ_0, healthy reservoirs creation rate, ω_0^{-1}, healthy reservoirs lifetime. In absence of any other interaction the equilibrium density of healthy reservoirs is $m^*_0 = \lambda_0 / \omega_0$. Healthy reservoirs are infected by their interaction with virions at a rate $\gamma_{\alpha\beta}\, \nu_{\alpha\beta}\, m_0$. Anti-$\alpha$ cytotoxic cells destroy infected reservoirs at a rate $p m_{\alpha\beta}\, x_\alpha$. (Anti-$\beta$ cytotoxic cells destroy infected reservoirs at a rate $q m_{\alpha\beta}\ \ y_\beta$). The full variation rate for the healthy reservoirs is $\gamma_{\alpha\beta} \nu_{\alpha\beta} m_0 - m_{\alpha\beta}\,(p x_\alpha + q y_\beta) - \omega_1 m_{\alpha\beta}$. c) $g_{\alpha\beta}$ virions creation rate in reservoirs, $\xi u_{\alpha\beta}$, virions creation rate in infected T-helper cells, $f_{\alpha\beta} z \nu_{\alpha\beta}$, virions destruction rate (by an extracellular hit, coordinated by T-helper cells) . Virions invade reservoirs at a rate $\gamma_{\alpha\beta}\, \nu_{\alpha\beta}\, m_0$. The full variation rate for virions is $g_{\alpha\beta} m_{\alpha\beta} + (\xi u_{\alpha\beta} - f_{\alpha\beta})z\nu - \gamma_{\alpha\beta} m_0 \nu_{\alpha\beta}$. d) Infected cells active cytotoxic precursor cells x_α (y_β) at a rate c_α (k_β). For an anti-α, x_α CTL cell, cytotoxicity is acquired by T-helper mediated activation at a rate $\eta c_\alpha m_{\alpha\beta} z$, or by T-helper mediated clonation at a rate $c_\alpha m_{\alpha\beta} xz$ (similar processes occur for an anti-β, y_β CTL cell. The full rate of the x_α (y_β) cytotoxic cells variation is $\eta c_\alpha z m_{\alpha^*} + c_\alpha z m_{\alpha^*} x_\alpha - \omega_2 x_\alpha\, (\eta k_\beta z m_{*\beta} + k_\beta z m_{*\beta} y_\beta - \omega_2 y_\beta)$.

as an outcome of the interaction of virions, $v_{\alpha\beta}$ healthy reservoirs, m_0, infected reservoirs, $m_{\alpha\beta}$ T-helper, *z*, and cytotoxic cells, x_α and y_β. Dynamics of our model is outlined in the Figure 1 and its detailed mathematical description is given in the appendix. All our variables mean densities. An antigen can simultaneously present several epitopes, but the immune system normally recognizes just one or two of them (36), so we shall only consider that virions display just two epitopes, *i* with two variants i_1 and i_2, and *j* also with two variants j_1 and j_2. We write $v_{\alpha\beta}$ for a virion exhibiting the variable α of the epitope *i*, and the variable β of the epitope *j*. Any set of healthy cells which is susceptible to be invaded by the virus, and then to produce viral particles will be called a reservoir, m_0. Reservoirs have a lifetime $(\omega_0)^{-1}$ and a creation rate of λ_0. A $v_{\alpha\beta}$-infected reservoir is $m_{\alpha\beta}$ and it lives $(\omega_1)^{-1}$. T-CD4 cells acting mainly as coordinators of the immune response are called *z*; they are created at a rate λ_z and they live a time $(\omega_z)^{-1}$. *Infected cells* elicit a response of cytotoxic cells (CTL) addressed against them. CTL directed against infected cells bearing the α variant of the epitope *i* are denoted by x_α, while those directed against cells bearing the variant β of epitope *i* by y_β. Cytotoxic cells live $(\omega_2)^{-1}$ and they are created for two different processes mediated by T-CD4 cells, activation, and clonation. A singular aspect of this model (shared by most of the current models for the interaction HIV-1-immune system) is that there is not any analytical way of dealing with it, so we must rely on numerical work for describing its properties. When we consider, however, just one viral variant, xx we found a null equilibrium point (no virions nor infected cells) given by:

$$m^*_0 = \frac{\lambda_0}{\omega_0}, z^* = \frac{\lambda_z}{\omega_z}, v^*_{11} = m^*_{11} = x^*_1 = y^*_1 = 0. \qquad [1]$$

This point is asymptotically stable if

$$h \equiv \frac{\lambda_z}{\omega_z}\left(f_{11} - \xi u_{11}\right) > \frac{\lambda_0}{\omega_0}\gamma_{11}\left(\frac{g_{11}}{\omega_1} - 1\right). \qquad [2]$$

2.2. Mutations

HIV-1 high mutability is associated to a defect in the inverse transcriptase process used by all retrovirus in the synthesis of viral DNA from RNA. Not all the mutations are significant ones, but just that fraction changing an existing epitope into a new one, not checked by cytotoxic cells. We used for our simulation a Montecarlo routine ruled by the kernel $R = \exp\left(-s\gamma_{\alpha\beta} n\Delta t\right)$, where *s* is a variable adjustment parameter which we call mutability, *n* is the number of elapsed time steps and Δt, the time step interval. *R* is compared to the output of a normalized generator of random numbers, *A* and each time that $R < A$, a mutation takes place. For $t \approx 0$, $R \approx 1$, therefore mutations are unlikely, while for a $t \to \infty$, $R \approx 0$ and some of the possible mutations occur. The fraction of virions produced each time is α. Some of the outputs of this mutation process are shown in the Figures 5, 6, and 7.

2.3. Opportunistic infection

We now consider the action of a non immunocytopatic agent ρ for simulating bacterial or tumor infections, which evolve as:

$$\frac{d\rho}{dt} = a\rho(1-\rho) - b\,\rho m_0 \qquad [3]$$

the logistic term takes into account a limited growth of the infected agent, and the last term, its uptake by a contact interaction with macrophages, at a rate *b*, refinements to this simple model are immediate. As a healthy immune system wipe out opportunistic infections, we took for our simulations $b \equiv \frac{\alpha\omega_0}{\lambda_0}$, and $a = 1$, other choices for *a* imply just a renormalization of our system of equations.

3. Results

We used an Euler expansion for working our resultant set of fourteen coupled ordinary differential equations. The outputs of some numerical integrations are shown in the following Figures 2 to 9.

3.1. Fulfillment of the conditions of equilibrium

We begin displaying the output of our integrator for the case with just one viral variable, v_{11}. Figure 2 shows system's variables behavior as a function of h for large values of time (50.000 computation steps). It is evident the fulfilling of the condition (9). Dashed lines represent a system obeying equations (1) to (6), with just a viral variable, v_{11}. We have also plotted (solid line) a system with $\gamma_{11} = 0$ in equations (1) and (6), and $p_1 = q_1 = 0$ in equations (3) and (4) (virions do not enter into reservoirs, and there is no CTL attack on them). The last situation seems to be unfavourable for the immune system. Now we consider situations with $h > \frac{\lambda_0}{\omega_0}\gamma_{ij}\left(\frac{g_{ij}}{\omega_1} - 1\right)$, this is, with strong immune response. Figure 3-a shows the temporal evolution of virions, v_{11}, and T-helper cells, z, for diverse initial values of both variables. The immune system keeps its grip over virus although the initial viral density is high in some simulations. Figure 3-b is virus, v_{11} vs. T-helper cells, z diagram. All the trajectories in this space converge toward the null equilibrium point. Fulfilling of equation (9) leads to T-CD4$^+$ cells permanence and control of the illness. A situation with weak immune response, $h < \frac{\lambda_0}{\omega_0}\gamma_{ij}\left(\frac{g_{ij}}{\omega_1} - 1\right)$, is shown in the Figure 4. Figure 4-a shows temporal evolution of the viral and T-helper cells densities. Note that virus emerges irrespective of the initial immune cells density. Figure 4-b is a virus, v_{11} vs. T-helper cells, z diagram. Our system seems to have a finite, and perhaps unstable, equilibrium point (this is suggested by

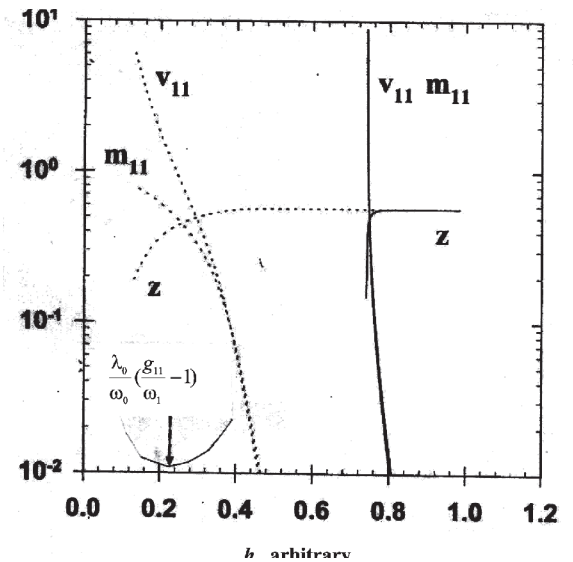

Figure 2. System's behavior for just a viral variant, v_{11}, with cytolithic attack on reservoirs (dashed lines) and in absence of such attack, with no infection to reservoirs (solid lines). We plotted virions, v_{11}, infected reservoirs, m_{11}, and T-CD4 helper cells, z. There occurs a shift in the convergence region from $h \cong 0.725$ to $h \cong 0.420$ but this shift of the null point is not caused by CTL attack on infected cells, but for virions invasion to reservoirs. CTL densities are negligible, and m_0 evolution roughly parallels that of z, so we did not plot these variables. We took for this and the remaining figures $\gamma_{11} = 0.35$, $g_{11} = 0.65$, $p_1 = q_1 = 4$, $c_1 = k_1 = 0.55$, $f_{11} = 4.9$, u_{11} 2.25, $\eta = 0.02$, $\lambda_0 = 0.25$, $\lambda_z = 4$, $\omega_0 = \omega_1 = 0.28$, $\omega_2 = 140$, and f, variable between 3.24 and 5.24.

he fact that all the trajectories in the (z, v_{11}) space converge toward a preferential one, but this trajectory is unbounded.

3.2. Effect of the mutations

Now we show the effect of mutations on the system's behavior. Figure 5 displays the

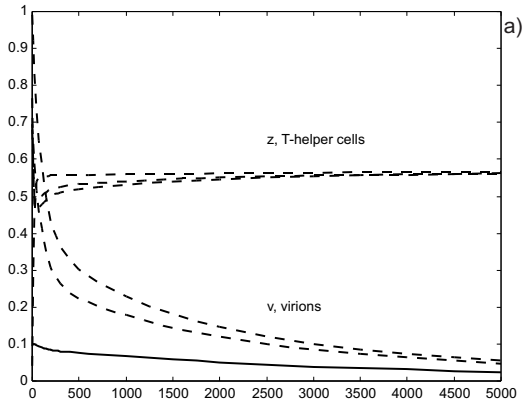

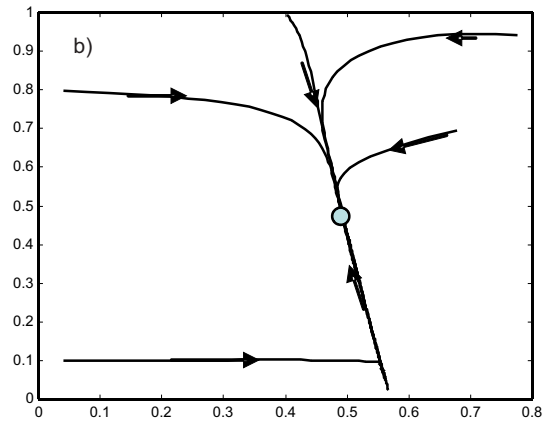

Figure 3. a) Temporal evolution of viral, and T-helper cells concentrations for a situation with $h_M > \frac{\lambda_0}{\omega_0}\gamma_{ij}(g_{ij}/\omega_1 - 1)$, strong immune response. Immune system controls every infection, irrespective of the initial inoculums. b) Plot of viral density ν_{11} vs. z, T-CD4 helper cells density. The stable equilibrium point is easily observed. We took identical values for the parameters to those in the Figure 2 but, $\omega_2 = 7$, and $\xi = 1.80$ ($h = 0.486$). The initial values for the variables were $m_0(0) = 0.89$, $m_{11}(0) = 0.10$, $x_1(0) = \gamma_1(0) = 0.10$, and the remaindering ones are seen from the figure.

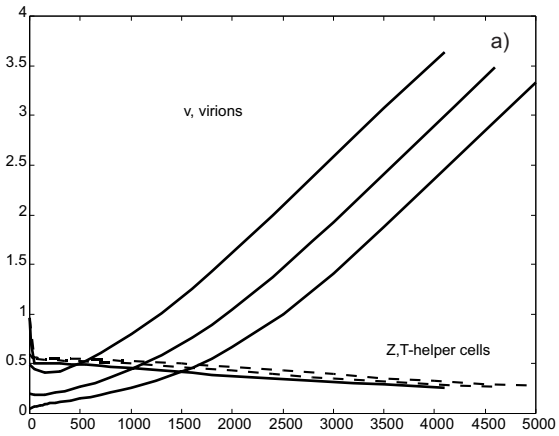

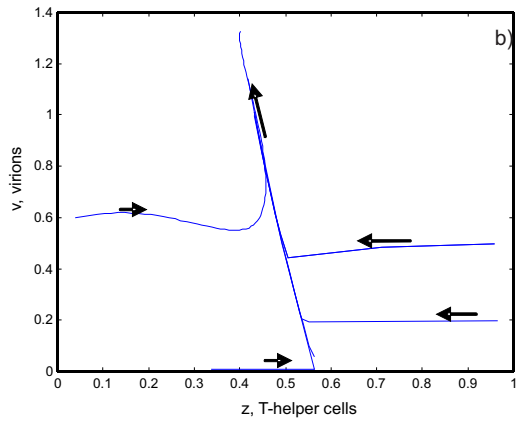

Figure 4. a) Temporal evolution of our system for $h > \frac{\lambda_0}{\omega_0}\gamma_{ij}(g_{ij}/\omega_1 - 1)$, weak immune response. Immune escape occurs irrespective of initial concentrations both of virions and T helper cells. b) Plot of viral density ν_{11} vs. z, T-CD4 helper cells density. All the trajectories seem converge toward a preferred one. This fact suggests the existence of an unstable equilibrium point. For the purpose of plotting we arbitrarily truncated all the curves. Parameters and initial values for the variables were identical to those in the Figure 3, but. $\xi = 2.10$ ($h = 0.100$).

values of total viral density, $\sum_{i,j} \nu_{ij}$, and z, T-CD4$^+$ cells density, as a function of h after 50000 steps of integration. Dotted lines represent a system with just a variable epitope, this is, with the presence of ν_{11}, ν_{12}, ν_{13} and ν_{14} variants. This implies that the epitope i (1) is always seen by CTL. Solid lines represent another situation with two variable epitopes, this is, with the presence of ν_{11}, ν_{12}, ν_{21} and ν_{22} variants, therefore a delay occurs since a viral mutation takes place until the production of specific CTL $x_i\left(y_j\right)$. This last situation is unfavourable for the immune system, requiring higher values of h for controlling viral emergence. In the Figure 6 we show the influence of rate of mutation on viral escape. We displayed there total viral density, $\sum_{i,j} \nu_{ij}$ as function of time for three different values of the mutability, s, and $h > \frac{\lambda_0}{\omega_0}\gamma_{ij}\left(\frac{g_{ij}}{\omega_1} - 1\right)$ for each viral variable ν_{ij} in all the instances, but with the presence of CTL attack on infected reservoirs. For low mutability, s= *0.01*, immune response controls infection. For moderate mutability, s= *0.1*, viral density slowly progress. For high mutability, s= *1.0*, virus has the advantage. The net outcome of viral high mutability is impairing CTL attack on infected reservoirs. Figure 7 is a map of the (h, s) space showing convergence (control of infection) and divergence (viral escape from immune control) regions. We used here a continuously mutant system with the ν_{11}, ν_{12}, ν_{21} and ν_{22} viral variants. For each value of α the immune system keeps a grasp on the infection in the region under each curve. Then, this figure displays convergence regions for a continuously mutant system. A more effectively mutant virus (higher α) has the advantage over the immune response. Saturation observed for high values of s shows that a too high rate of mutation does not supply a more advantageous situation for virus.

3.3 Effect of CTL parameters

Figure 8 shows the influence of CTL activity on control of viral progression for three instances of the $\frac{\omega_2}{\omega_z} = \frac{\tau_{TCD4}}{\tau_{CTL}}$ ratio (remember that $\tau = \omega^{-1}$ represents the lifetime of an entity). Strength of CTL attack on infected reservoirs is measured by p_i and q_j parameters, whilst activation rate of CTL is measured by c_i and k_j (we took $p_i = q_j$, and $c_i = k_j$ for all these simulations). Any point on each curve represents the minimal value of p_i (q_j) necessary for obtaining immune control (finite, non null, non diverging values of viral variables ν_{ij} and m_{ij}) for a given $c_i\left(k_j\right)$ after 50.000 computation steps. There exists control of the infection in the region outside each curve, so we call them activation curves. Note that CTL permanence (lower $\frac{\omega_2}{\omega_z}$ ratio) as an activated entity addressed against a fixed epitope facilitates immune task (lower values for the parameters $p_i, q_j, c_1 k_j$). From the figure is seen that each one of these curves are bounded and closed, and therefore there is an attraction valley containing them. Additionally, this figure shows that the product of $p_i\left(q_j\right)$ times $c_i\left(k_j\right)$ parameters, that is, CTL activation rate times infected reservoirs clearance rate is the relevant factor for controlling infection viral. Note, finally that our curves also empirically show the existence of a non null but non progressing equilibrium point.

3.4. Opportunistic breakthrough

Figure 9 shows the result of our simulations after an opportunistic invasion ruled by the equation (3). A healthy organism easily controls the additional, non cytopathic infection (continuous lines), but a system with weakened immune system is overwhelmingly infested by the opportunistic agent (dotted lines). Thus our system correctly reproduces the well known fact that on advanced stages

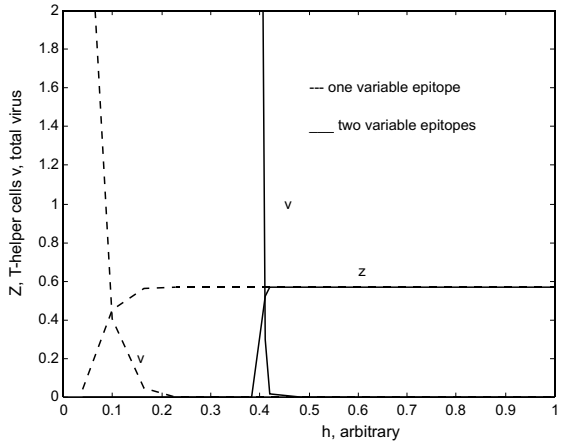

Figure 5. Comparison between system behavior for a case with a fixed epitope ($\nu_{11}, \nu_{12}, \nu_{13}$ and ν_{14} variants) (dashed line) and other one with two variable epitopes ($\nu_{11}, \nu_{12}, \nu_{21}$, and ν_{22} variants) (solid line). We plotted total viral density, $\nu_{TOT} = \sum_{i,j} \nu_{ij}$ (or $\sum_{i1j} \nu_{1j}$) and *z*, T-CD4 helper cells vs. h_M, immune response. Immune system is disarticulated by the presence of two continually mutant epitopes (note the rightward shift for the convergence region for the last situation). We took $\omega_2 = 2\omega_z = 14$, $1 \le \xi \le 3$, and the remaining parameters identical to those in Figure 2.

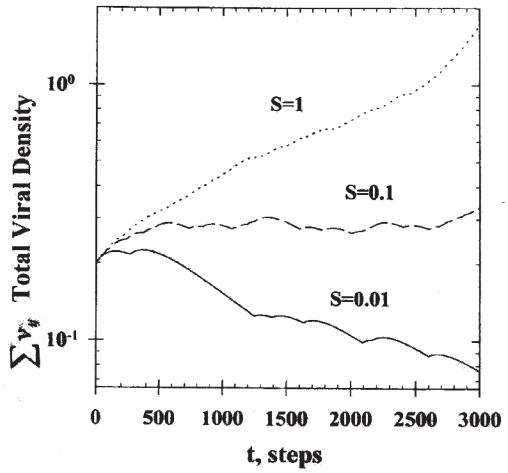

Figure 6. Time evolution of total viral density $\sum_{i1j} \nu_{1j}$ for diverse values of the mutability *s*. Mutation is ruled by a Montecarlo kernel $S = \exp(-s\gamma_{ij} n\Delta t)$, *n* is the number of steps in arbitrary units of time, Δt, and *s* is the mutation rate. For $s = 0.01$, low mutability, virions are quickly wiped out by immune system. For $s = 0.1$, moderate mutability, viral density oscillates before slow growth. After mutations (marked by changes in the slope of the curves) there are transient increases in the viral density caused by the current delay in CTL specific response. For $s = 1.0$, high mutability, total virions density diverges.

of AIDS infection opportunistic agents invade the weakened organism.

4. Discussion and Conclussions

The behavior of our system's null equilibrium point is shown in the Figure 2. Equation (3) is fulfilled by the system, and this fact suggests that the convergence threshold could become arbitrarily minute by making $\gamma_{\alpha\beta} \to 0$, blocking virions invasion to reservoirs, a technic suggested in Gigere and Tremblay (38) and Zhang et al (39), (this fact also means $u \to 0$, stopping of viral infectivity to T-CD4 cells) and/or $g_{11} \to 0$ (stopping virions production in reservoirs), and/or $\omega_1 \to \infty$ (lengthening life time of active CTL in the blood stream). Alternatively, *f* (antibody mediated virions attack) could make high, but this seems to be a difficult issue, not only for the lacking of a secure way of signalling viral epitopes for destruction, but also by the existence of escape mechanisms from antibodies control (28). Virion invasion to reservoirs has been described since long time, but some aspects of this invasion and

later behaviour of the virus inside this host are not yet fully understood, and we think that these important subjects should be revisited. Current therapy make stress in impairing the synthesis of viral DNA from RNA and also the assembling of viral particles (blocking viral integrases) (40), that is, in making $\xi \to 0$ and $g_{\alpha\beta} \to 0$. This goal could also be reached attacking viral RNA directly, not just the proteins it encode (41, 42). Temporal evolution of virions and T-helper cells is shown in Figures 3 and 4. Figure 3 shows the desired but not yet achieved situation of immune control. T-helper cells concentration, z remains constant and virions v_{ij} fade. Figure 4-a agrees with the current behaviour of VIH-1 infection: viral breakthrough and decline of T-helper cells concentration. Some interesting questions arise from Figure 4-b. Numerical work suggest that our system seems to have a finite, and perhaps unstable, equilibrium point. Could this hypothetical equilibrium point be made both stable and as small as desired? Could the flux toward that point become as slow as desired? We found situations with no divergence after more than 50.000 computation steps (in fact we used such points for assembling our bordering curves in Figure 8). So, numerical work suggests that the answer is yes. We recall that there exist no analytical way to answer to these questions. On the other side, therapy has reported cases of non progressing seropositives (43).

Mutation is a hallmark of all retrovirus and it poses a hard challenge to the immune system. If CTL do retain their grasp on a viral epitope, they keep their check of the viral breakthrough, a fact observed from the Figure 5. Note that viral control occurs first in the system with a non-mutating viral epitope, irrespective of the number of existing viral variables. Figure 6 shows that higher rate of mutability results in viral advantage. Viral escape occurs by impairment of CTL attack on infected reservoirs. This fact seems agree with reports stating that viral breakthrough precedes viremia (44). Once viral escape is well established, a further growth in the viral mutation rate does not supply an additional viral advantage (Figure 7). The saturation of viral production in our model could also be rooted in the limited number of viral variables on it (v_{11}, v_{12}, v_{21}, and v_{22}), or by the so-called diversity catastrophe (45). The existence of activation curves bounding regions of viral advantage is apparent in Figure 8. This figure also shows that for controlling vi-

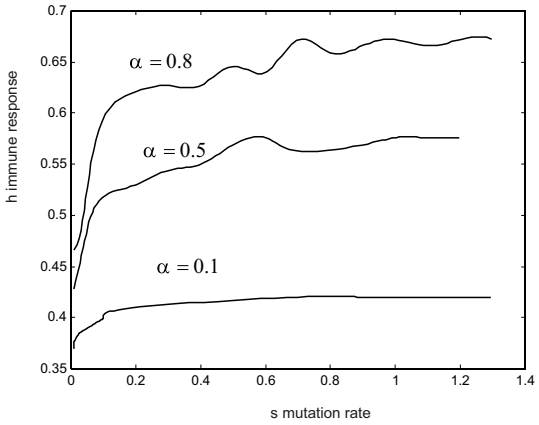

Figure 7. Space of convergence h_M vs. s for a continually mutant system. α is the fraction of significant viral mutants produced each time a mutation occurs. For each value of α the system has control of infection in the region below the curve $\alpha = cte$ Note that 1) For low and moderate values of s, the immune response intensity required for controlling infection grows exponentially. 2) The higher the fraction α of significant variants produced, the higher must be the immune response. 3) For high s values, there occurs saturation of the viral diversity, and a further growth in s, mutability rate, does not provide an additional advantage to the virus.

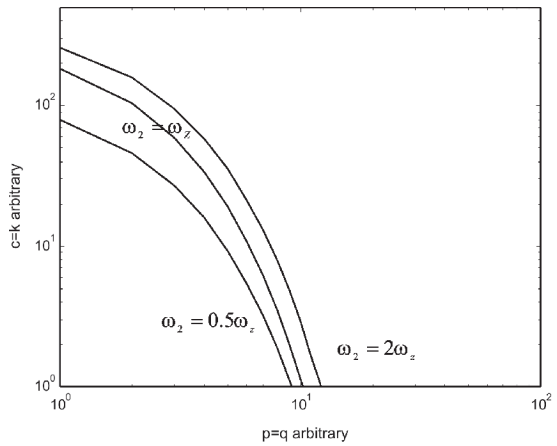

Figure 8. Immune response activation curves for some values of the $\omega_2 / \omega_z = \tau_{TCD4} / \tau_{CTL}$ ratio. Ordinate axis represents the value of the parameters $c_i = k_j$ necessary for obtaining system's convergence. Abscise axis has similar meaning for the parameters $p_i = q_j$. Points forming all the curves had minute, but non null values for viral densities after 50.000 computational steps. Each curve delimits the lower boundary of a convergence region; this is, for a value of the ratio ω_2 / ω_z there is immune control in the region placed to the left of the respective curve. Permanence of activated CTL (measured by their meantime) facilitates immune task. We took $s = 0.5$ and $\alpha = 0.10$, and the remaining parameters, the same as in Figure 2. Initial values for the variables were $m_{ij}(0) = v_{ij}(0) = 0.10$, $x_i(0) = y_j(0) = 0.05$, $m_0(0) = 0.89$, $z(0) = 0.57$.

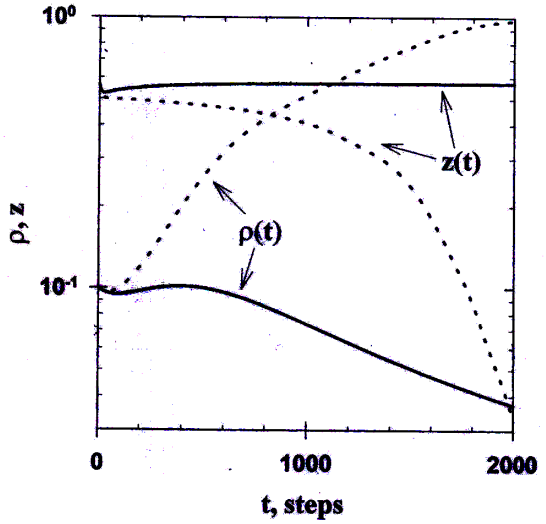

Figure 9. Time evolution of the opportunistic agent ρ and T-helper cells z for viral control (solid line) and viral outgrowth (dashed line). Infection develops as a consequence of decrease of immune cells density. A healthy organism easily controls the invasion, but a weakened organism

ral infection, the product $p_i(q_j)$ times $c_i(k_j)$ parameters must be high. Then, CTL activation rate times infected reservoirs clearance rate is the important quantity for controlling the infection viral. This fact seems to be a common sense rule, but it poses a hard task on CTL: they not only must be created in a sufficient high rate, but also they must have reasonable and continuous antiviral performance. Opportunistic infection is just a consequence of a diminution of the density of immunocompetent cells caused by viral attack on them. We conclude that our model not only reproduces several well stated facts related to the progression from VIH-1 infection to AIDS, but also suggests an alternative for fighting this progression, namely by the control of the productive viral invasion to reservoirs.

Aknowledgements

Dr. Miguel Martin-Landrove (Centro de Resonancia Magnética, Facultad de Ciencias, Universidad Central de Venezuela) gave enthusiastic support and advice during all the stages of this work, Miss Ana Medina drew

the Figure 1, and Miss Carla Ortega Di Gregorio performed the idiomatic revision.

References

1. FINZI D., HERMANKOVA M., PIERSON M., CARRUTH L., BUCK C., CHAISSON R., QUINN T., CHADWICK K., MARGOGLICK J., BROOKMEYER R., GALLANT J., MARKOWITZ M., HO D., RICHMAN D., SICILIANO R. ***Science*** 278:1295-1300, 1997.
2. ORENSTEIN J., FOX C., WAHL S. ***Science*** 276: 1857-1861, 1997.
3. CHUN T., FAUCI A. ***Proc Natl Acad Sci USA*** 96: 10958-10961, 1999.
4. TENNER-RACZ P., RACZ M., DIETRICH M., KERN P. ***The Lancet*** J12**:** 105-106, 1985.
5. PANTALEO G., GRAZIOSI C., BUTINI L., PIZZO P., SCHNITTMAN S., KOTLER D., FAUCI A. ***Proc Natl Acad Sci USA*** 88: 9398-9842, 1991.
6. PANTALEO G., GRACIOZI, C., DEMAREST J., BUTINI L., MONTRONI M., FOX C., ORENSTEIN J., KOTLER D., FAUCI A. ***Nature*** 362: 355-362, 1993.
7. DYBUL M., WEISSMAN D., RUBBERT A., MACHADO E., COHN M., EHLER L., O'CALLAHAN M., MIZELL S., FAUCI A. ***AIDS Res and Human Retrovirus*** 14: 1109-1113, 1998.
8. BOUNOU S., LECLERC J., TREMBLAY M**.** ***J Virol*** 76: 1004-1014, 2002.
9. SATO H., ORENSTEIN J., DIMITROV D., MARTIN M. ***Virology*** 186: 712-724, 1992.
10. KLENERMAN P., PHILLIPS R., RINALDO C., WAHL L., OGG G., MAY R., MC MICHAEL A., NOWAK M. ***Proc Natl Acad Sci USA*** 93: 15323-15328, 1996.
11. LEVY J. ***Microbiol Rev*** 57: 183-289, 1993.
12. MONTEFIORI D., HILL T., VO H., WALKER B., ROSENBERG E. ***J Virol*** 75: 10200-10207, 2001.
13. HART M., SAIFUDIN M., SPEAR G. ***J Gen Virol*** 84: 353-360, 2003.
14. OGG G., KOSTENSE S., KLEIN M., JURRIANS S., HAMANN D. MC MICHAEL A., MIEDEMA F. ***J Virol*** 73: 9153-9160.
15. SCHMITZ J., KURODA M., SANTRA S., SASSEVILLE V., SIMON M., LIFTON M., RACZ P., TENNER-RACZ K., DALESANDRO M., SCALLON B., GHRAYEB J., FORMAN M., MONTEFIORI D., RIEBER P., LETVIN N., REIMANN K. ***Science*** 283: 857-860, 1999.
16. BORROW P., LEWICKI H., HAHN B., SHAW G., OLDSTONE M. ***J Virol*** 68: 6103-6110, 1994.
17. GOULDER P., PRICE D., NOWAK M., ROELAND-JONES S., PHILLIPS R., MC MICHAEL A. ***Immunol Rev*** 59: 17-29, 1997.
18. ARNAOULT R., NOWAK M., WODARZ D. ***Proc R Soc London B*** 267:1347-1354, 2004.
19. GRAY C., LAWRENCE J., SCHAPIRO J., ALTMAN J., WINTERS M., CROMPTON M., LOI M., KUNDUM S., DAVIS M., MERIGAN T. ***J Immunol*** 162: 1780-1788, 1999.
20. YANG O., KALAMS S., TROCHA A., CAO A., LUSTER A., PAUL JOHNSON R., WALKER B. ***J Virol*** 71: 3120-3128, 1997.
21. KALAMS S., GOULDER SHEA A., JONES N., TROCHA A., OGG G., WALKER B. ***J Virol*** 73: 6721-6728, 1999.
22. WODARZ, D., NOWAK, M. ***Phil Trans R Soc Lond B*** 355: 1059-1070, 2000.
23. WICK D., SELF S. ***J Theor Biol*** 219: 19-31, 2002.
24. WODARZ D., MAY R., NOWAK M. ***Int Immunol*** 12: 467-477, 2000.
25. WAHL L., BITTNER B., NOWAK M. ***Int Immunol*** 12: 1371-1380, 2000.
26. STEINMAN R., GERMAIN R**.** ***AIDS*** 12: (suppl. A) S97-S112, 1998.
27. SATTENTAU Q., MOULARD M., BRIVET B., BOTTO F., GUILLEMOT J., MONDOR I., POIGNARD P., UGOLINI S. ***Immunol Letters*** 66: 143-149, 1999.
28. WEI X., DECKER J., WANG S., HUI H., KAPPES, J., WU X., SALAZAR-GONZALEZ J., SALAZAR M., KIRBY M., SAAG M., KOMAROVA N., NOWAK M., HAHN B., KWONG P., SHAW G. ***Nature*** 42:307-312, 2003.
29. CHIEN Jr. P., COHEN S., TUEN M., ARTHOS J., DE CHEN P., PATEL S., HIOE C. ***J Virol*** 78: 7645-7652, 2004.

30. MOIR S., LAPOINTE R., MALASPINA R., OSTROWSKI M., COLE C., CHUN T., BASELER M., HWU P., FAUCI A. ***J Virol*** 73: 7972-7980, 1999.

31. JUNG A., MAIER R., VARTANIAN J., BOCHAROV G., JUNG V., FISCHER U., MEESE E., WAIN-HOBSON S., MAYERHANS W. ***Nature*** 418: 144, 2002.

32. DE BOER R., PERELSON A. ***J Theor Biol*** 190: 201-214, 1998.

33. WODARZ D., NOWAK M. ***Bioassays*** 24: 1178-1187, 2002.

34. NOWAK M., MAY R. ***Virus Dynamics, Mathematical principles of Immunology and Virology*** Oxford University Press, N.Y. pp. 1-250, 2000.

35. ORTEGA H., MARTÍN-LANDROVE M**.** ***Act Cien Venez*** 55: 247-263, 2004.

36. NOWAK M., MAY, R., PHILLIPS R., ROWLAND-JONES S., LALLO D., MC ADAM S., KLENERMAN P., KÖPPE B., SIGMUND K., BANGHAM C., MC MICHAEL A. ***Nature*** 375: 606-611, 1995.

37. WAHL S., ORENSTEIN J. ***J Leuk Biol*** 62: 67-71, 1997.

38. GUIGERE J., TREMBLAY M. ***J Virol*** 78: 12062-12065, 2004.

39. ZHANG M., XIAO, X., SIDOROV I., CHOUDRY V., CHAM F., ZHANG P., BOUMA P., ZWICK M., CHOUDARY A., MONTEFIORI D., BRODER C., BURTON D., QUINNAN, Jr. G., DIMITROV D. ***J Virol*** 78: 9233-9242, 2004.

40. HAZUDA D., FELOCK P., WITMER M., WOLFE A., STILLMOCK K., GROBLER J., ESPESETH A., GABRIELSKI L., SCHLEIF W., BLAU C., MILLER D. ***Science*** 287: 646-650, 2000.

41. DAVE R., POMERANTZ R. ***J Virol*** 28: 13687-13696, 2004.

42. KAMEOKA M., NUKUZUMA S., ITAYA A., TANAKA Y., OTA K., IKUTA K., YOSHIHARA K. ***J Virol*** 78:8931-8934, 2004.

43. QUINN T., WAVER M., SEWANKAMBO N., SERWADDA D., CHUANJUN L., WABWIRE-MANGEN F., MEECHAN M., LUTALO T., GRAY R. ***The NE Jour Med*** 342: 921-929, 2000.

44. FEENEY M., TANG Y., ROOSEVELT K., LESLIE A., MCINTOSH K., KARTHAS N., WALKER B., GOULDER P. ***J Virol*** 78: 8927-8930, 2004.

45. SOLÉ R., DEINSBOECK T**.** ***J Theor Biol*** 228: 47-54, 2004.

Appendix

We begin by introducing the following symbols:

$$m_{\alpha\cdot} = \sum_j m_{\alpha j} \qquad m_{*b} = \sum_i m_{ib}$$

$$(uv)^* = \sum_{i,j} u_{ij} v_{ij} \quad (\gamma_{\alpha\beta} v_{\alpha\beta})^* = \sum_{i,j} \gamma_{ij} v_{ij},$$

Dynamics of the healthy reservoir cells is described by:

$$\frac{dm_0}{dt} = \lambda_0 - (\gamma_{\alpha\beta} v_{\alpha\beta})^* m_0 - \omega_0 m_0. \qquad \text{[A-1]}$$

The equation for the infected reservoir cells evolution is:

$$\frac{dm_{\alpha\beta}}{dt} = \gamma_{\alpha\beta} v_{\alpha\beta} m_0 - m_{\alpha\beta}(px_\alpha + qy_\beta) - \omega_1 m_{\alpha\beta}. \qquad \text{[A-2]}$$

Dynamics of the cytotoxic cell densities are described by:

$$\frac{dx_\alpha}{dt} = \eta c_\alpha z m_{\alpha\cdot} + c_\alpha z m_{\alpha\cdot} x_\alpha - \omega_2 x_\alpha. \qquad \text{[A-3]}$$

$$\frac{dy_\beta}{dt} = \eta k_\beta z m_{*\beta} + k_\beta z m_{*\beta} y_\beta - \omega_2 y_\beta. \qquad \text{[A-4]}$$

The equation for the T-CD4+ cells is:

$$\frac{dz}{dt} = \lambda_z - (uv)^* z - \omega_z z. \qquad \text{[A-5]}$$

The equation for the virions is:

$$\frac{dv_{\alpha\beta}}{dt} = g_{\alpha\beta} m_{\alpha\beta} + (\xi u_{\alpha\beta} - f\alpha\beta) z v_{\alpha\beta} - \gamma_{\alpha\beta} m_0 v_{\alpha\beta}. \qquad \text{[A-6]}$$